Lund, Andreas E.D.

Effect of heat and mass transfer related parameters on the performance of deep borehole heat exchangers

Published in:
Applied Thermal Engineering

DOI:
10.1016/j.applthermaleng.2024.123764

Published: 15/09/2024

Document Version
Publisher's PDF, also known as Version of record

Applied Thermal Engineering 253 (2024) 123764

Contents lists available at ScienceDirect

Applied Thermal Engineering

journal homepage: www.elsevier.com/locate/apthermeng

Research Paper

Effect of heat and mass transfer related parameters on the performance of deep borehole heat exchangers

Andreas E.D. Lund [a]

[a] *Department of Electrical Engineering and Automation, Aalto University, FI-00076 Aalto, Espoo, Finland*

ARTICLE INFO

Keywords:
Deep borehole exchanger
Geothermal heat
Heat pump
Heat transfer
Mass transfer
Sector coupling

ABSTRACT

Deep borehole heat exchangers (DBHE) are a highly potential clean heat source. Using 3-D numerical simulations, a comprehensive analysis on the effect of design parameters and geological conditions for 1–3 km deep DBHEs were undertaken. Key parameters included the inner and outer pipe diameter of the well, insulation between them, borehole depth, mass flow rate, and thermal conductivity and geothermal temperature gradient of ground. The whole heating system performance with the DBHE, heat pump, and circulation-pump-unit of the well was also analyzed. The results show that the performance of the well is strongly influenced by its design and mass flow rate with increasing well depth. For a 1 km to 3 km DBHE, the thermal output ranges from 46 kW to 240 kW at steady state in Scandinavian conditions. A smaller inner pipe in the well could increase the output by 7–11 % compared to a larger pipe, but a higher mass flow rate could produce even 75 % more heat than a lower one. However, the effect of the inner pipe and mass flow rate would be the opposite on the whole energy system efficiency when considering the COP of a heat pump connected to well and the well pressure losses. The geological conditions of the rock have a major effect, too.

Nomenclature

Symbols	
A	m^2. cross section area
c_p	$J\ kg^{-1}K^{-1}$. specific heat capacity
d	m. diameter
d_h	m. hydraulic diameter
f_d	–. friction factor
G	$^oC\ km^{-1}$. geothermal temperature gradient
h	$W\ m^{-2}$. heat transfer coefficient
I	–. iteration
L	m. length of the pipe
$\dot{m}$	$kg\ s^{-1}$. mass flow rate
Q	W. power
Q'	$W\ m^{-1}$. heat flux per unit length (heat source)
Q''	$W\ m^{-1}$. external heat exchange through pipe wall
p	Pa. pressure
R	$m\ K\ W^{-1}$. thermal resistance
t	s. time
T	K. temperature
u	$m\ s^{-1}$. fluid velocity
U	$W\ m^{-1}\ K^{-1}$. U-value
Z	m. wall perimeter
α	K^{-1}. coefficient of thermal expansion
β	K^{-1}. coefficient of volumetric expansion

(*continued on next column*)

(*continued*)

Symbols	
η	–. pump efficiency
η_{CA}	–. Carnot non-ideality factor
η_m	–. mechanical efficiency of compressor
λ	$W\ m^{-1}\ K^{-1}$. thermal conductivity
ρ	$kg\ m^{-3}$. density
Φ	W. thermal power of the heat pump system
μ	Pa s. dynamic viscosity
Subscripts	
c	conduction
com	compressor
cond	condenser
evap	evaporator
g	ground
f	fluid
syst	system
Abbreviations	
BHE	Borehole exchanger
CHP	Combined heat and power
COP	Coefficient of performance
DBHE	Deep borehole heat exchanger
DH	District heating
FEM	Finite element method
HP	Heat pump

(*continued on next page*)

E-mail address: andreas.lund@aalto.fi.

https://doi.org/10.1016/j.applthermaleng.2024.123764
Received 25 June 2023; Received in revised form 21 May 2024; Accepted 19 June 2024
Available online 21 June 2024

(*continued*)

Symbols	
EU	European Union
GSHP	Ground-source heat pump
Nu	Nusselt number
Pr	Prandtl number
PtH	Power-to-heat
Re	Reynolds number

1. Introduction

The Paris Climate Agreement calls for major emission cuts to limit the global warming to 1.5 °C, which will require net-zero emissions by the middle of this century [1]. Many nations have responded to this challenge by launching new policies and policy measures to reach carbon neutrality. For example, the European Union (EU) has started a massive set of actions under its Green Deal programme aiming at carbon neutrality by year 2050 [2].

Though the efforts needed to cut the emissions will cover the whole energy sector, the heating and cooling sectors will play a central role in this context as at least half of all final energy consumption comes from the thermal energy use [3,4]. More specifically, considering the built environment, the household heating and hot water consumption e.g. in Finland accounts for close to 80 % of the total household energy use [5]. In cold climates notable shares of the heating is delivered through district heating (DH) schemes enabling versatile means of heat production, e.g., combined heat and power (CHP), renewable energy sources, waste heat, and heat pumps, among others, which could help to reduce the emissions. For example, in Denmark, DH stands for over 60 % of all heating [6,7] and in Finland for more than 40 % [8]. In these countries CHP schemes are widely employed with DH, e.g., in Finland two-thirds of the district heating is produced through co-generation [5]. A major challenge for large older CHP plants is that they may still rely on fossil fuels, and shifting the fuel use to clean energy sources such as biomass is not always possible because of the large demand of fuel imposing challenges to supply logistics. For example, in Helsinki, the capital of Finland, over 90 % of all heat is produced through DH and CHP, but with fossil fuels. The city needs some 7 TWh of heat supply [9] which should be turned into zero-emission solutions in less than a decade to meet the climate goals of Finland [9].

Electrification of the heating sector offers a promising approach for decarbonizing heating, when employing zero-emission electric production. For example, in the Nordic countries the whole power sector is envisioned to reach zero-emissions by 2030 [10]. Thus, employing Power-to-Heat (PtH) conversion through heat pumps could be a possibility to decarbonize heat supply. Heat pumps are commercially available also in larger scale, e.g., for cities, feeding heat into the district heat network or for single buildings [11,12]. Heat pumps can use various types of heat sources, e.g., waste, ambient heat, or ground heat [13]. For urban use with restricted space, ground-source heat pumps (GSHPs) could serve both space heating and cooling of buildings through employing the ground as a source and sink of thermal energy [14]. Importantly, the thermal inertia of the ground enables a much smoother operation of the heat pump, e.g., compared to air-source heat pumps which show lower performance in the winter-time due to a lower coefficient of performance in cold conditions [15].

Considering large-scale heat pump schemes for urban regions and buildings, the planning of the heat source for the heat pump needs special consideration to avoid under- or oversizing of the system which could lead to suboptimal and costly systems. For example, traditional borehole exchangers with a depth up to 300–400 m [16,17], which are often used for single houses, may not be adequate for large heating schemes as many wells would be required. This could cause thermal shielding leading to inefficient use of some parts of the ground heat source. In a Finnish case, a single non-constrained well extracted 108 kWh m^{-1} of heat in a year, but when employing multi-well schemes, the adjacent wells in an infinite field may produce just 30 kWh m^{-1} a^{-1} [18]. Though the real performance of ground coupled heat pump systems will vary with the local geological conditions, operational strategies, etc., and the above values are hence indicative only, traditional borehole exchanger design in densely built urban environment may not be adequate and improved solutions would be necessary.

To overcome this inherent limitation of traditional ground-coupled heat pump systems, deep borehole heat exchangers (DBHE) in ground, also called deep-heat wells, have been suggested [19]. Such deep boreholes could extend down to a few kilometers [19], which enables to extract much more heat than with the traditional wells [16]. For example, Kohl et al. [20] studied the operation of a 2302 m DBHE connected to a heat pump for building heating and found that the borehole could provide 0.39–0.49 MWh m^{-1} heat in a year. Wang et al. [21] showed that a heat pump with a 2 km DBHE could achieve a very high system COP of 4.5. Lund [22] simulated the performance of 2 km DBHE and found that in Finnish conditions the thermal output of one such DBHE would correspond to some thirty 300-m holes and would thus better fit urban use with space limitations than the traditional shallow borehole exchanger. The better performance per unit length of the DBHE originates not only from less interference between the boreholes, but also from the natural geothermal heat gradient, i.e., increasing ground temperature vis-à-vis depth, which improves both the heat yield and the COP of the heat pump.

Traditional shallow borehole exchanger and DBHE have been studied both analytically and numerically in several studies [23–25]. Piipponen et al. [19] used finite element modeling for borehole heat exchanger simulations and Zanchini et al. [23] implemented a finite element model for a coaxial borehole heat exchanger using the COMSOL Multiphysics® software package. In the present study, the finite element method was chosen using COMSOL Multiphysics® software.

The study by Zanchini et al. [23] on coaxial borehole heat exchangers examined the impact of thermal short-circuiting, flow rate, material composition, and geometric configuration of boreholes. However, the study was limited to boreholes with a depth of 100 m. Luo et al. [24] studied deep borehole heat exchangers and performed a thermal analysis on varying borehole depth from 200 to 800 m and varied the position of the inlet and outlet pipes, but excluded deeper geological conditions and employed an analytical approach. Holmberg et al. focused on coaxial BHEs and their performance ranging from 200 to 1000 m in depth [25].

Piipponen et al. [19] have investigated the operation of deep borehole heat exchangers with depths ranging from 800 to 2000 m in different parts of Finland focusing on the influence of geothermal properties. The thermal conductivity of the bedrock was varied between 3.19 Wm^{-1}K^{-1} and 3.30 Wm^{-1}K^{-1}, and the geothermal temperature gradient from 13 °C km^{-1} to 13.9 °C km^{-1}. For example, in Central Europe, the geothermal gradient can reach up to 40 °C km^{-1}, whereas in Finland, it can be 20 °C km^{-1} or lower. The study also examined the effects of different materials of the inner pipe of the coaxial pipe, specifically comparing vacuum-insulated tubing (VIT) and high-density polyethylene pipe (HDPE). However, in their comparison, different dimensions were used for the VIT pipe and HDPE, resulting in an incomplete comparison of the impact of the material and dimensions.

Thermal analysis of 1–3 km deep DBHEs is highly topical as these are now starting to penetrate to the heating market, e.g., in the Nordic countries: two 1.5 km deep boreholes in Norway [26] and one pilot system with a 1.3 km deep borehole in Finland [27] have been realized. At the same time, the local conditions of deeper holes may much differ from the traditional low-depth boreholes (e.g. 300 m), e.g. the temperature levels are much higher and thermal short-circuiting may occur. Finding optimal design range for DBHE wells is therefore important, which is also a subject of this paper.

Though the above studies provided detailed thermal analysis both on the DBHE and heating systems linked to boreholes, they did not provide a complete systematic analysis on the effects of the key borehole

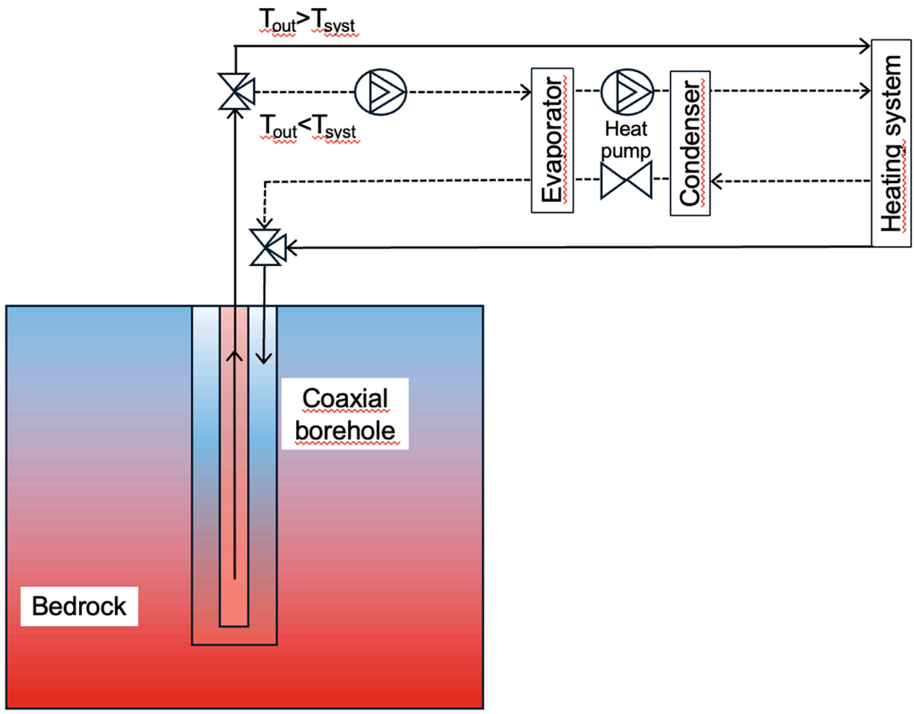

Fig. 1. Principle of deep borehole heat exchanger heating system.

parameters such as flow conditions, borehole structure, dimensions, and geology, which are the subject of this study. In addition, these studies often utilized technical parameter values from pre-commercial pipes. However, when developing innovative technologies, such as DBHE, considering a broader parameter value range is important when seeking for optimal solutions. An example of such development would be coaxial pipes for DBHE with different dimensions, also dealt with in this paper. Moreover, the depth of the borehole and other design parameters such as the dimensions of the inner and outer pipes used in the previous case studies differ from those considered here, e.g., the depth of the DBHE ranges here from 1 km to 3 km.

The main aim of this paper is to determine how different design parameters such as borehole heat exchanger pipe dimensions and insulation affect the performance of 1 km – 3 km deep DBHEs and to find optimal well configurations for different operational conditions and local geology. These research questions are investigated through detailed numerical simulations of heat and mass transfer in the well which is thermally coupled to the surrounding ground. A novel feature of the present modelling approach is the more detailed description of the heat transfer and mass flow in the borehole heat exchanger also enabling more accurate design optimization of the DBHE. Though some of the heat pump system analysis with the borehole heat exchanger system is performed for Finnish conditions, the parameter variation analyses also provide insight to other conditions, e.g., in northern Europe. The analysis considers both the performance of the well alone and its effect on the performance of the heat pump in the heating system. The approach considering the DBHE, heat pump and circulation-pump of the well as a whole provides novel insight on how their interactions affect the energy performance and DBHE sizing.

The paper starts with a description of the deep borehole heat exchanger well in Section 2 followed by Section 3 showing the theoretical model of the well and the key input data used in the analyses. In Section 4, the main results are presented. The paper ends with conclusions in Section 5.

2. Principle of deep borehole heat exchanger

A deep borehole heat exchanger differs from a conventional borehole exchanger through three major features: The depth of the borehole in ground, the type of heat collector-pipe used, and the liquid circulating in the borehole. A deep borehole heat exchanger exhibits higher heat extraction capacity compared to a conventional shallow borehole not only because of the larger depth but also due to the higher rock temperature originating from the geothermal gradient. For example, in traditional BHE, either a U-tube (closed system) or a coaxial pipe (open or closed system) are used, whereas in a DBHE a coaxial pipe is normally employed [25,28]. In a closed circulation system, an antifreeze solution (e.g., alcohol-water mixture) could be employed allowing sub-zero temperatures and extracting heat at lower temperatures, but the heat transfer between the fluid and ground is lower than in an open system. In the coaxial system, water is used as the circulation fluid as the outer surface is typically in contact with ground. In this study a coaxial well in an open system is employed, typical for DBHE.

The principle of the deep borehole heat exchanger heating system is illustrated in Fig. 1. The DBHE can be run in two modes depending on the outlet temperature from the borehole: (1) If the outlet temperature is higher than that required for heating ($T_{out} > T_{syst}$), then the heat from the borehole can be directly utilized for heating. This could be possible when e.g. the geothermal temperature gradient is high, the borehole is very deep or the mass flow rate in the borehole is low; (2) if the temperature is not high enough ($T_{out} < T_{syst}$), then a heat pump will be needed to raise the temperature to the required level. Due to the lower geothermal temperature gradient used here, the DBHE in this paper will be used as a heat source for a heat pump system to raise the return water temperature from the well to a useful level needed in the application, which would be typically from 75 to 120 °C in a traditional district heating network [29]. However, if employing low-temperature heat distribution principles, the temperature level could be substantially dropped e.g. to 50–80 °C. A low system temperature would be preferable as it would increase the efficiency of the DBHE coupled heating system, both in case of direct and heat pump assisted use.

A detailed illustration of the coaxial DBHE or ground heat exchanger

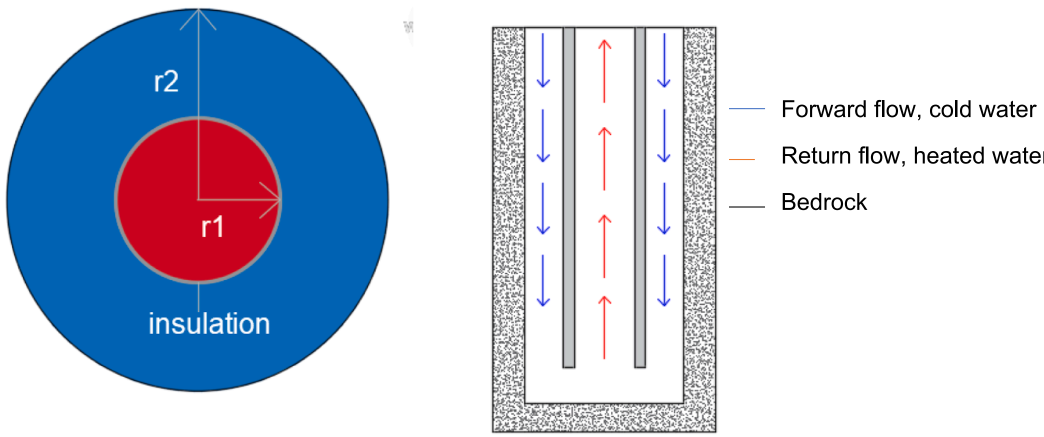

Fig. 2. Illustration of a coaxial borehole heat exchanger. Left: Cross-section showing the structure of the well (blue = cold fluid, red = warm fluid). Right: Fluid circulation in the borehole (grey = area between r_1 and r_2 which is the insulation).

is shown in Fig. 2. The DBHE consists of an inner and outer pipe. The operation of a DBHE is simple: cold water from the return flow of the heating system or the heat pump evaporator circuit is injected along the outer pipe, which extracts heat from the ground, and the heated water is returned through the inner pipe to the heating system or heat pump which raises the temperature to the level required by the building or district heating network. These fluid flow directions represent the optimal flow scheme in a well [25,30].

The water flowing in the outer pipe section is in direct contact with the bedrock. The heat transfer between the inner and outer pipe with downward and upward water flows can be reduced either by using insulation between the pipes avoiding thermal short circuiting, e.g. vacuum insulation tubing or by increasing the mass flow of the water circulated in the DBHE [31]. For this reason, the coaxial pipe is particularly suitable for deeper borehole exchangers. The coaxial pipe is designed to utilize a larger proportion of the borehole's cross-sectional area as the flow area. As a result, it allows for a higher mass flow rate to be employed. By using a coaxial pipe in deeper boreholes, higher mass flow rates can be achieved without significant pressure loss increasing the heat extraction capacity of the deep borehole heat exchanger. In contrast, in a conventional shorter BHE, it will be challenging to increase the mass flow rate without increasing the pressure loss ($\Delta p \sim u^2$), which would necessitate increasing the pumping power resulting in higher pumping power and reducing the overall efficiency of the DBHE.

The depth of a DBHE is typically from 1 km to 3 km [25,29–31] compared to traditional shallow BHE with a depth up to 400 m [22]. In the present study, it is assumed that the topmost 300 m of the DBHE is cased to avoid any interaction with the surrounding environment, e.g., ground water [19]. Below this level, the well is uncased, and the coaxial well is in direct contact with the adjacent rock thus assuming that the rock is intact preventing water leakage from the hole to the bedrock.

A DBHE could also be used for heat storage through reversing the flow directions. If adding to the system in Fig. 1 an external heat source with a temperature exceeding that of the ground at the bottom of the borehole, e.g. industrial waste heat or surplus electricity through a power-to-heat scheme, then reversing the flow direction in the well would regenerate the ground, which would also function as a heat storage. Hot water would in this case be fed along the inner tube into the well and the return water in the outer pipe heats up the ground and cools down before entering the ground surface. If the hot water were injected into the ground along the outer pipe, the fluid immediately starts to heat up the ground and the cooled water flows down with a risk that it could even cool the lowest part of the well, which is avoided through the proposed flow arrangement [32]. This paper deals with heat extraction from the well only.

3. Methodology

In the next, the theoretical basis of the DBHE is presented which is used in simulating the well performance. Thereafter, the input parameters used are defined including defining the key variables used for studying the effects of heat and mass transfer.

3.1. Modelling of deep borehole heat exchanger

The heat and mass transfer in the ground is modelled in 3D for a geometry shown in Fig. 2. The heat transfer in the ground is governed by heat conduction in a solid. No ground water flow through the well system is assumed. The borehole is coupled to the heat transfer through a source/sink term (Q'). The heat transfer equation of ground can then be written as follows [33]:

$$\rho_g c_{p,g}\frac{\partial T_g}{\partial t} = \lambda_g \nabla^2 \mathrm{T}_g + Q' \times (dxdy)^{-1} \tag{1}$$

where $c_{p,g}$ = specific heat capacity of the ground (J kg^{-1} K^{-1}), ρ_g = density of ground (kg m^{-3}), λ_g = thermal conductivity of ground ($Wm^{-1}K^{-1}$), T_g = temperature of the ground (K), $\acute{Q}$=heat source/sink per unit-depth (dz) in vertical direction (Wm^{-1}), and dx, dy = unit-lengths in x and y directions, respectively. For simplicity, we have omitted the vector representation of the 3D variables in Eq. (1).

The heat transfer in the borehole is assumed to be one-dimensional in vertical direction and it comprises of two components: heat transfer in the pipe annulus and in the inner pipe. The heat transfer in the pipe is dominated by convection. The fluid temperature T_f (z) in the pipe can be solved from the energy balance equation of an incompressible fluid flowing in the pipe [34]:

$$\rho_f A c_{p,f}\frac{\partial T_f}{\partial t} + \rho_f A c_{p,f} u \nabla T_f = \nabla \bullet (A \lambda_f \nabla T_f) + f_D \frac{\rho A}{2d_h}|u|^3 + Q' + Q'' \tag{2}$$

where A = pipe cross section area for flow (m^2), $c_{p,f}$ = specific heat capacity of the fluid ($Jkg^{-1}K^{-1}$), d_h = hydraulic diameter (m), f_D = friction factor, λ_f = thermal conductivity of the fluid ($Wm^{-1}K^{-1}$), $\acute{Q}$= heat source/sink term (Wm^{-1}), $\acute{Q}$= external heat exchange through pipe wall (Wm^{-1}), u = fluid velocity in the pipe (m^{-1}), ρ_f = fluid density (kg m^{-3}).

The mass transfer is coupled to the heat transfer through the fluid velocity term u in Eq. (2), which is an exogenous variable. The term $\acute{Q}$ thermally couples the borehole with the ground and is subject to the following boundary condition:

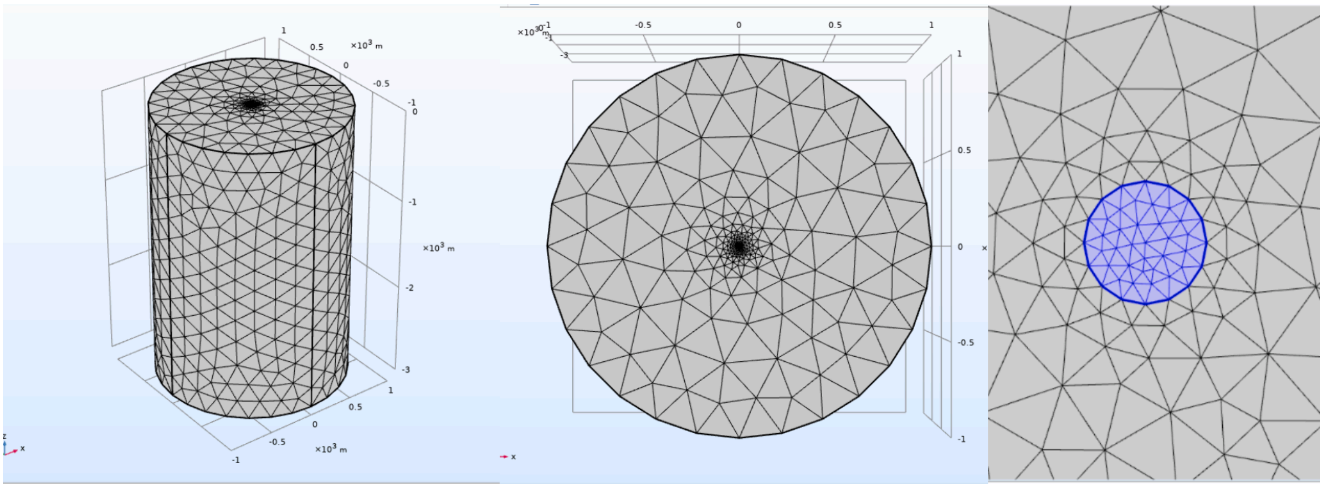

Fig. 3. Example of the computational network (normal mesh density) used in the simulation of the well. Left: Overall view of the mesh; Center: cross-sectional view; Right: surroundings of the borehole with a finer mesh.

$$Q' = 2\pi r_2 \lambda_g \left(\frac{\partial T_g}{\partial r}\right) 2\pi r2\, h(T_f - T_g)|r = r_2 \tag{3}$$

where h = heat transfer coefficient between the ground and pipe fluid ($Wm^{-2}K^{-1}$), r_1 = radius of the inner pipe of the DBHE (see also Fig. 2), r_2 = outer radius of the DBHE. The heat transfer coefficient (h) can be determined with the help of the Nusselt number (Nu) [32]:

$$h = \lambda_f d_h^{-1} Nu \tag{4}$$

To calculate the Nusselt number, the Gnielinski-correlation is employed [35]:

$$Nu = \frac{\left(\frac{f_D}{8}\right)(Re - 1000)Pr}{1 + 12.7\left(\frac{f_D}{8}\right)^{\frac{1}{2}}\left(Pr^{\frac{2}{3}} - 1\right)} \tag{5a}$$

$$\mathrm{Pr} = \frac{c_{p,f}\mu}{\lambda_f} \tag{5b}$$

where Pr = Prandtl number, μ = dynamic viscosity.

The term $\acute{Q}$ describes the thermal coupling of the inner and outer pipes of the DBHE as follows:

$$Q'' \times dz = 2\pi r_1 R^{-1}(T_{f1} - T_{f2}) \tag{6}$$

where R = thermal resistance between the pipes (=1/U-value) (m K/W), T_{f1} = fluid temperature in the inner pipe (K) and T_{f2} = fluid temperature in the outer pipe (K).

Equation (6) shows that if R is low, thermal short-circuiting between the pipes may occur. This can be avoided by using an insulated inner pipe, i.e., the thermal resistance between the pipes R is large and hence $\acute{Q} \approx 0$ [36,37].

Eqs. (1)-(6) form the set of equations that describe the thermal performance of the well and its surroundings. The equations are numerically solved with the COMSOL-Multiphysics® 6.0 software [38]. An important part of the numerical model is the definition of the computing network or mesh [16]. The computing time and computer memory needed for solving the physical model with the finite element method used in COMSOL is very much affected by the type of mesh chosen and the number of mesh elements. Several alternatives for the computational mesh were considered including physics-controlled quadratic shaped elements, and user-defined triangular and tetrahedral geometries with three element densities (course/normal/dense). Here a combined triangular- tetrahedral network with a normal density (12192 elements) was chosen which gave an adequate accuracy with a reasonable computing time. For the fluid in the borehole, 40 vertical elements were used. A single 25-year simulation took 25–30 min on a MacBook Pro © computer with Apple M2 processor and 16 Gb core memory. Ten-folding the number of elements to over 120,000 would improve the accuracy of the simulations by $<$ 5 % but increases the computing time 5-fold. Huang et al. reported on similar experiences with a refined mesh with 4-fold number of elements leading to less than 1 % improvement [51]. The COMSOL model was earlier successfully validated [22] against another numerical model [25] which was used also here as reference for the accuracy assessment.

Fig. 3 illustrates the mesh used for the simulation which consists of several thousands of element points. The computing grid is denser around the borehole and gets coarser further off. Typically, the spatial dimension of the simulated volume (x, y, z) is 2 km x 2 km x 1 km + borehole depth to minimize the effects from the boundaries of the mesh. At the boundaries of the physical model mesh, which were set distant enough to avoid interaction between the borehole heat exchanger and the boundaries of the model, the normal heat flux was set to zero. This indicates that no heat can traverse these boundaries. In practice, the thermal impact from the borehole will not reach the boundaries during the 25-year simulation period.

The geothermal temperature gradient is incorporated into the model as an initial value of the ground temperature. The vertical ground temperature is set at t = 0 as $T_g(z) = T_g(z_0) + G \times (z\text{-}z_0)$ $(z > z_0)$, where G is the geothermal temperature gradient and $T_g(z_0)$ is the ground temperature corresponding to the depth z_0 not anymore affected by the ambient (here we used T_g (z_0) = 6.8 °C at z_0 = 10 m which is typical for Southern Finland), i.e. the fluctuating temperature of the topsoil layer is neglected. This is justified by its very small portion of the total DBHE length, and the insulation used around the upper part of the borehole. The $T_g(z)$-profile applies to all temperature values in the (x,y)-plane at the respective depth z.

The DBHE performance is evaluated at steady state at t = 25 years with continuous heat withdrawal from the well. Fig. 4(a) illustrates how the steady state is approached when a 2 km DBHE is discharged continuously with a constant mass flow rate (9 kg s^{-1}). The output from t = 0 to t = 25 years drops by ca 45 % in this case, but at t = 25 years the yearly power output changes less than 1 % indicating full steady state. The temperature development around the well is illustrated in Fig. 4(b) and 4(c) showing that the 'cold pulse' spreads to ca 35 m from the well, which also sets the minimum distance of wells in a multiple-well system in this case. The development of the temperature contours in Fig. 4(d) shows that steady-state in the ground is reached close to t = 25 years,

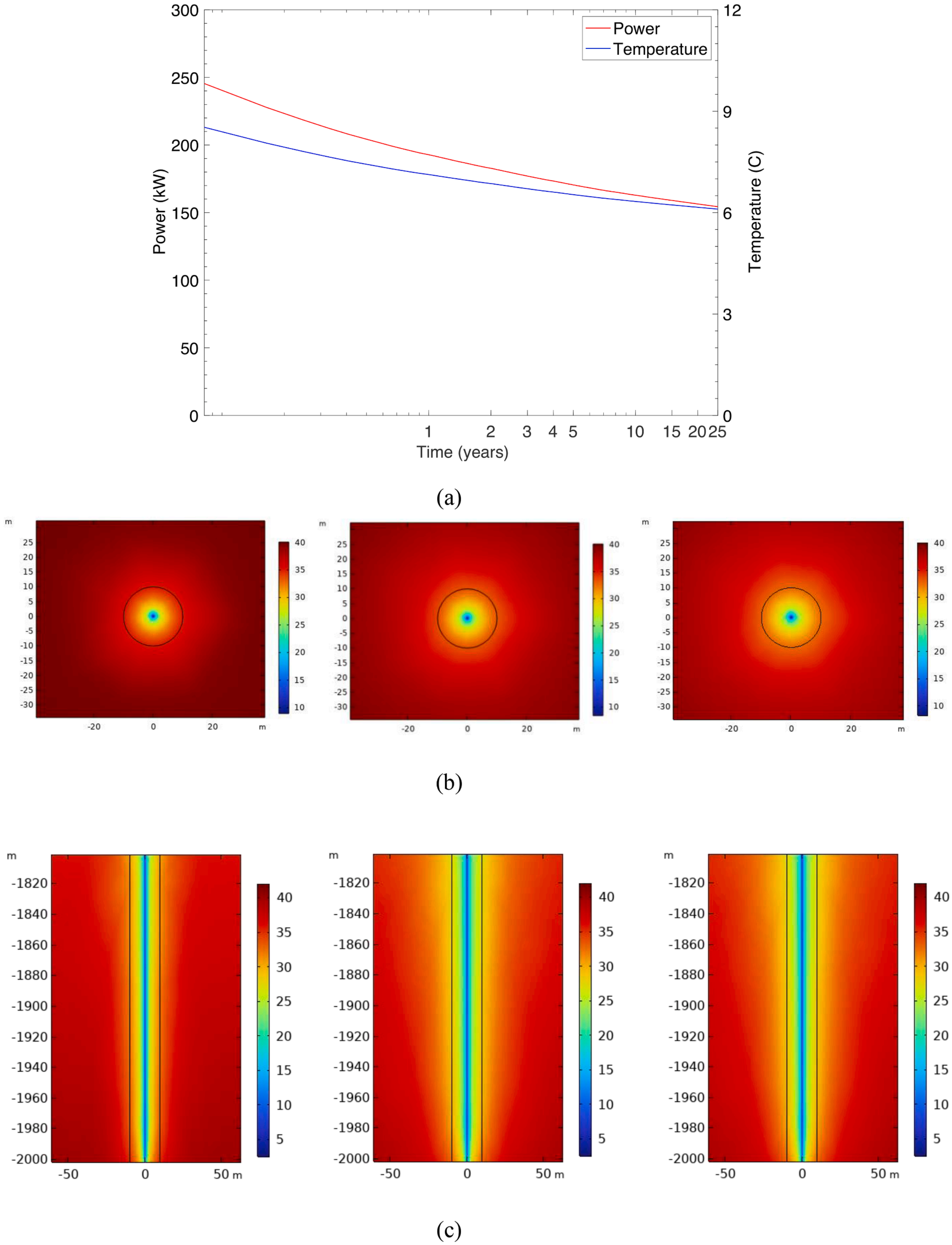

Fig. 4. (a) Temporal change of output power and outlet temperature from a 2-km DBHE well. (b) spatial temperature distribution $T_g(x,y, z = 2\text{ km})$ around the well after 5, 15 and 25 years of discharging (from left to right), (c) cross-sectional temperature distribution $T_g(x = 2\text{ km}, y, z)$ around the well after 5, 15 and 25 years of discharging (from left to right), (d) development of temperature contours around the well at 1 km (left) and 2 km (right) depth. $\lambda_g = 3\ \mathrm{Wm^{-1}K^{-1}}$, $2r_2 = 200$ mm, $G = 20\ ^\circ$C/km.

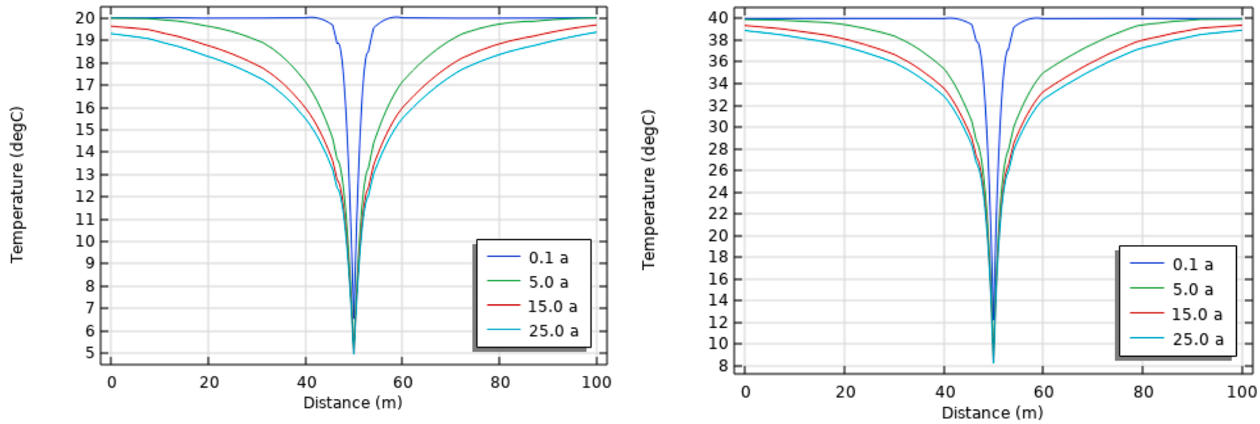

(d)

Fig. 4. (*continued*).

thus justifying the choice of the time point t = 25 years for the length of the simulations.

Coupling to heat pump

The inlet temperature of the fluid fed into the well is determined by the application. Typically, the heat well is coupled to a heat pump, which uses the well as a heat source. The system layout of the heat pump system was illustrated in Fig. 1. The outlet temperature from the evaporator of the heat pump is then set as the inlet temperature of the fluid in the well, i.e., $T_{in} = T_f(t,0)$. The inlet to the evaporator is connected to the outlet of the well, i.e. $T_{out} = T_f(t,L)$. Then, the thermal power from the well to the heat pump system (Φ) can be calculated as follows:

$$\Phi = \dot{m}c_p(T_{out} - T_{in}) \tag{7}$$

where$\dot{m}$ = the mass flow rate corresponding to the fluid velocity u in the pipe (kg s^{-1}), T_{in} = inlet temperature of the fluid to the well (^{o}C), T_{out} = outlet temperature of the fluid from the well (^{o}C),

To determine T_{out}, the performance of the heat pump need to be considered. Based on the energy conservation law, the high-temperature condensing heat of the heat pump (Q_{cond}) equals to the low-temperature evaporation heat (Q_{evap}) plus the compression power (Q_{comp}), i.e., $Q_{cond} = Q_{comp} + Q_{evap}$. The Coefficient of Performance COP describes the efficiency of the heat pump as follows [39,40]:

$$COP_{HP} = \frac{Q_{cond}}{Q_{comp}} \tag{8}$$

The COP of the heat pump depends on the operating conditions, and it can be approximated as follows [41]:

$$COP_{HP} \approx \eta_{CA}\eta_m \frac{T_{cond}}{T_{cond} - T_{evap}} \tag{9}$$

where η_{CA} = Carnot non-ideality factor (0.45–0.55), η_m= mechanical efficiency of the compressor (0.90–0.95) [41], T_{cond} = condensing temperature (K), T_{evap} = evaporating temperature (K). The temperature of the heat source and application cannot be directly used in Eq.(9) because of the heat losses in the heat exchanger and piping, and the non-ideal heat transfer to the heat pump. The condensing and evaporating temperatures need typically to be adjusted by ΔT = 5–10 K, i.e., the condensing temperature = application temperature + ΔT and the evaporation temperature = heat source temperature-ΔT [41].

The coupling of the DBHE and the heat pump takes place through three terms: $T_{in} = T_f(t,0)$, $T_{out} = T_f(t,L)$, and the fluid flow in the pipe (u), which affect the delivered heat and the COP of the heat pump. T_{in} is determined by the heat pump performance and internal set values, and it is handled exogenously in the modelling, e.g., here T_{in} is set to 2 °C.

There is an additional loss factor which need to be considered in DBHE, namely the pressure losses, which will influence the power need of the circulation pump. The electricity needed for the pumps will in turn affect the total system performance. To account for theses parasitic losses, we defined a system COP considering the pumping power for the fluid flow in the wells (Q_{pump}):

$$COP_{system} = \frac{Q_{evap} + Q_{comp}}{Q_{comp} + Q_{pump}} = COP_{HP} \times \frac{Q_{comp}}{Q_{comp} + Q_{pump}} = \frac{COP_{HP}}{1 + \frac{Q_{pump}}{Q_{comp}}} \tag{10}$$

The pumping power can be estimated from the pressure losses in the borehole as follows [42]:

$$\Delta p = 0.5 f_d L d_h^{-1} \rho_f u^2 \tag{11}$$

$$Q_{pump} = \rho_f^{-1} \eta^{-1} \Delta p \dot{m} \tag{12}$$

where L = pipe length (m), Δp = pressure drop (Pa), η = pump efficiency. The frictional heat generated through the pressure loss is negligible and has no effect on the fluid temperature.

There is a trade-off between the pumping power and the thermal output from the well: Increasing the flow rate will increase the thermal output from the well, but also the pumping power requirement, and vice versa. Also, a higher flow rate will decrease the outlet temperature from the well, and hence the COP of the heat pump, and vice versa. Thus, the overall system performance of the DBHE system is a result of several interacting factors, which are analyzed in Section 4.

3.2. Parameters and input values

For the performance analysis, the effect of the following set of key geological and well parameters is investigated in more detail:

- Deep borehole heat exchanger parameters: Well depth, mass flow rate, inner and outer pipe diameter, insulation between the inner and outer pipe.
- Geological parameters: Geothermal temperature gradient, thermal conductivity of the bedrock.

In the reference case, the following parameter values are used: Depth of well 2000 m, diameter of inner pipe 90 mm, diameter of outer pipe 200 mm, insulation of inner pipe 0.4 $Wm^{-1}K^{-1}$ (HDPE, standard high-density polyethylene) [43], geothermal temperature gradient 20 °C/km, thermal conductivity of ground 3 $Wm^{-1}K^{-1}$. The U-value of the insulation of the inner pipe is varied between 0.02 $Wm^{-1}K^{-1}$ to 0.4 $Wm^{-1}K^{-1}$. The value of 0.02 $Wm^{-1}K^{-1}$ corresponds to vacuum insulated pipe

Table 1
Range of parameter values used in the analysis.

Parameter	Range	Unit
Depth	1000–3000	m
Inner pipe diameter	80, 90, 100	mm
Outer pipe diameter	180, 200, 220	mm
Insulation of inner pipe (U-value)	0.02, 0.2, 0.4	W m^{-1} K^{-1}
Geothermal temperature gradient	15, 20, 30	^{o}C km^{-1}
Thermal conductivity of ground	2, 3, 4	W m^{-1} K^{-1}

and 0.2 $Wm^{-1}K^{-1}$ to polypropylene or PVC. Table 1 gives the range of parameter values used in the analyses.

The geothermal temperature gradient depends on the local conditions. In Central Europe, typical values are 20–45 °C/km [37] and even beyond these in the volcanic areas. For instance, in France, the predominant gradient is around 30°C/km, but it approaches 50°C/km in some regions [46]. In Croatia, a typical gradient is 30-45°C/km, but in some places, it can be as low as 5°C/km or as high as 73°C/km [47]. Similarly, in the Scottish West Orkney basin, the gradient can locally vary from 20.6 to 37.1 °C/km [49]. In active volcanic regions the gradient may exceed 100 °C/km [52]. The geothermal temperature gradient in Scandinavia is typically 15-20°C/km, but sites with 30 °C/km are also found, e.g., in the Baltics [48]. The geothermal temperature gradient in Finland varies from 8 °C/km to 25 °C/km [36]. The reference geothermal temperature gradient is set here to 20 °C/km, which is typical to the Finnish bedrock [44,48]. The surface temperature is set at 6.8 °C which is the average ambient temperature for the case here (Southern Finland). The vertical ground temperature is initially set to its natural temperature value according to the geothermal temperature gradient as described earlier in the methodology section.

Another geological parameter of importance is the thermal conductivity of rock, which is influenced by several factors such as mineral composition, porosity, water content, etc. [50]. Thermal conductivity of rocks falls usually in the range of 0.4–7 W m^{-1} K^{-1}, where the lower values are typical to dry, not consolidated sedimentary rocks, and the higher values for sedimentary and metamorphic rocks; the quartz contents increases the thermal conductivity, even above 7 W m^{-1} K^{-1} is possible with very high contents. Claystone and siltstone falls in the range of 0.80–1.25 W m^{-1} K^{-1}, sandstones 2.5–4.2 W m^{-1} K^{-1}, and crystalline granite rock 3–3.5 W m^{-1} K^{-1} [49,50]. The intrusive bedrock in Finland typically has a thermal conductivity of 2–4 $Wm^{-1}K^{-1}$ [44,45].

A high geothermal temperature gradient and high thermal conductivity of the ground is advantageous for the energy performance of the DBHE. How their thermal interplay will influence the performance of the DBHE will be investigated in more detail in Section 4 (Results), but from the heat transport relation ($\lambda_g \nabla T_g$) it is evident that a drop in either of these factors would reduce the DBHE performance. For example, based on a test simulation of the DBHE, reducing the gradient from 45 °C km^{-1} to 20 °C km^{-1} decreased the average heat output by 47 % at 1 km depth and 55 % at 3 km at t = 25 years ($\lambda_g = 3$ W m^{-1} K^{-1}, $\dot{m}$=6 kg s^{-1}). A lower thermal conductivity would decrease the heat flow in the bedrock and thus also the thermal power of the DBHE. Depending on the type of rock and geological conditions, a combination of high geothermal temperature gradient and thermal conductivity could in principle be possible, at least in some parts of the borehole [53]. Several other factors of the ground also influence the suitability of a site for DBHE, e.g. ground porosity and tectonic stability. The Finnish bedrock considered here is in general well suitable for a coaxial DBHE without lining despite the somewhat modest geothermal gradient.

The mass flow rate used in the DBHE is varied from 6 kg s^{-1} to 15 kg s^{-1} and the inlet temperature of water is set to 2 °C, representing the outlet temperature from the heat pump, which can be kept constant through internal control of the HP. Lower temperatures than the set value can pose risks of freezing.

Besides investigating the effects of the parameter range on the well performance given in Table 1, the effects on the operation of the heat pump connected to the well will also be analyzed in Section 4.

4. Results

4.1. Effect of deep borehole heat exchanger parameters

In the next, the effects of the well depth, well flow rate, diameter of the inner pipe of the well and the heat transfer (insulation) between the outer and inner pipes of the well are investigated. The effects of the outer diameter on the performance within the studied range (180–220 mm) turned out to be very small for which reason a detailed analysis is not presented here.

Variation of the inner diameter.

The effect of varying the diameter of the inner pipe (return flow) in the coaxial borehole heat exchanger is illustrated in Fig. 5. The outer pipe diameter ($2r_2$) is kept constant at 200 mm. The ground has $\lambda_g = 3$ W m^{-1} K^{-1} and the geothermal temperature gradient is G = 20 and 30 °C km^{-1}.

Fig. 5 clearly shows that increasing the mass flow rate in the pipe will increase the output power but decreases the output temperature of the fluid as the output power increases less than the mass flow rate. A higher thermal gradient in the ground (Fig. 5(a) vs. Fig. 5(b)) yields higher power output and temperature which is very close proportional to the higher thermal gradient (1.5 x). The thermal output of a 2-km well at steady-state would be ca 100–200 kW (G = 20 °C km^{-1}) depending on the mass flow rath and inner pipe diameter – the higher values corresponding to the higher flow rate.

Considering the G = 20 °C km^{-1} case in Fig. 5(a), the diameter of the inner pipe has little effect on the outlet power or temperature from the pipe at depths below 2000 m and a mass flow rate 6 kg s^{-1}. For deeper holes, the 80 mm pipe yields 3–4 % higher output than the 100 mm one (Fig. 5(a)). Increasing the mass flow rate to 9 kg s^{-1}, the 80 mm pipe gives 2–3 % higher output at 1000–3000 m than the 100 mm pipe. Raising the mass flow to 15 kg s^{-1} causes differences in the output between the different pipe diameters already at shallow depths. For example, at 1000 m, the 80 mm pipe produces 11 % more power than the 100 mm pipe, but the difference drops to 7 % at 3000 m.

These results indicate that employing a smaller inner pipe diameter (for the range considered here) improved the thermal performance of the well. This can be explained through a couple of factors: Firstly, the heat transfer in the pipe is enhanced as the flow velocity increases; secondly, a smaller inner pipe helps in avoiding thermal short-circuiting as the distance between the cold and warm fluid flowing the pipes increase.

On the other hand, though a smaller inner pipe in this case improved the heat extraction from the well, the overall system effectiveness may not improve, e.g. due to increased pressure losses in the pipe which increase the electricity consumption of the circulation pumps discussed later in the paper.

Comparison of the absolute power output at different mass flow rates and well depths shows that using the 80 mm pipe at 15 kg s^{-1} yields 75 % higher output at 1000 m than at 6 kg s^{-1}, but the difference reduces to 60 % at 3000 m. When using a 100 mm pipe, the corresponding percentages are 57 % and 54 %, respectively.

The output temperature of fluid in Fig. 5 shows that the differences between the different pipe diameters increase with increasing well depth. The effect of the flow rate on the outlet temperature behaves inversely to the flow and the smallest pipe diameter provides the highest temperature, though the differences between the different pipe diameters are small.

The higher output power and fluid temperature with a higher geothermal temperature gradient in Fig. 5(b) means that the mass flow rate could be lowered to reach the same output level than with a smaller thermal gradient, or alternatively, a shallower borehole could be used, but this benefit decreases with shorter pipes. For example, 9 kg s^{-1} with

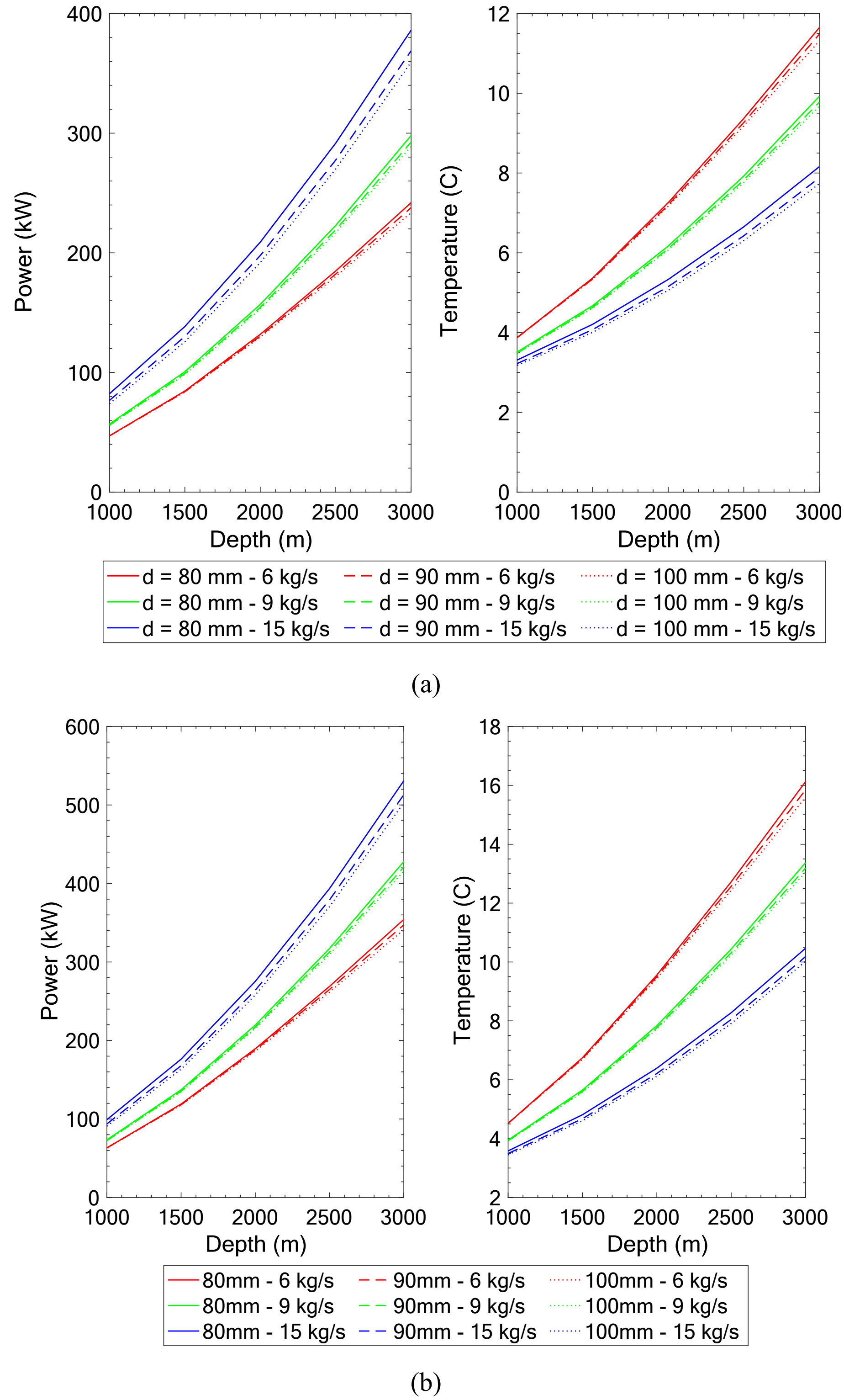

Fig. 5. (a) Effect of well depth, mass flow rate and inner pipe diameter on the extracted power (left) and on the outlet temperature (right). $\lambda_g = 3$ W m^{-1} K^{-1}, $2r_2 =$ 200 mm, G = 20 °C km^{-1}. (b) the same as (a) but G = 30 °C km^{-1}.

G = 20 °C km^{-1} corresponds to 15 kg s^{-1} with G = 15 °C km^{-1}.

As a conclusion of the above analysis, the smaller inner pipe diameter (80 mm) yields the best thermal power output from the well, but the difference to the other pipe diameters (90 mm, 100 mm) is very small at lower mass flow rates and well depths. At higher mass flow rates and/or deeper boreholes, the differences would increase to around 10 %. The effect of the other factors such as the fluid temperature and the pumping losses will be analyzed in Section 4.3 enabling a whole system view on the optimal pipe diameter.

Insulation between inner and outer pipe.

Next the effect of the thermal contact between the inner and outer pipe of the borehole heat exchanger was investigated by varying the U-value of the lining of the inner pipe. The results in Fig. 6 show that the thermal interaction between the two pipes, or forward and return flows

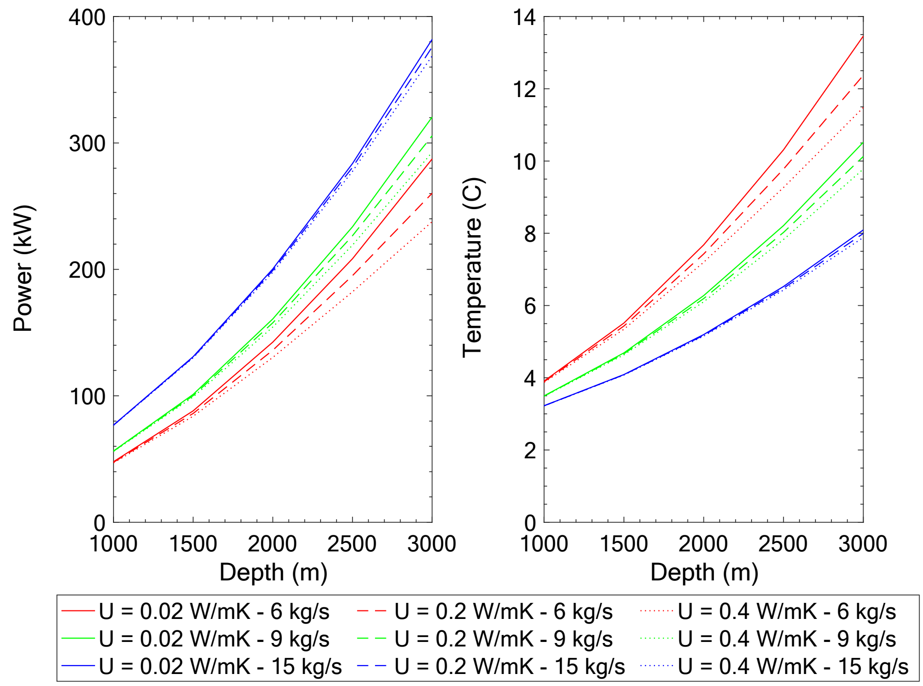

Fig. 6. Effect of insulation between the inner and outer pipe on the extracted power (left) and on the outlet temperature (right). $\lambda_g = 3$ W m^{-1} K^{-1}, $2r_1 = 90$ mm, $2r_2 = 200$ mm, $G = 20$ °C km^{-1}.

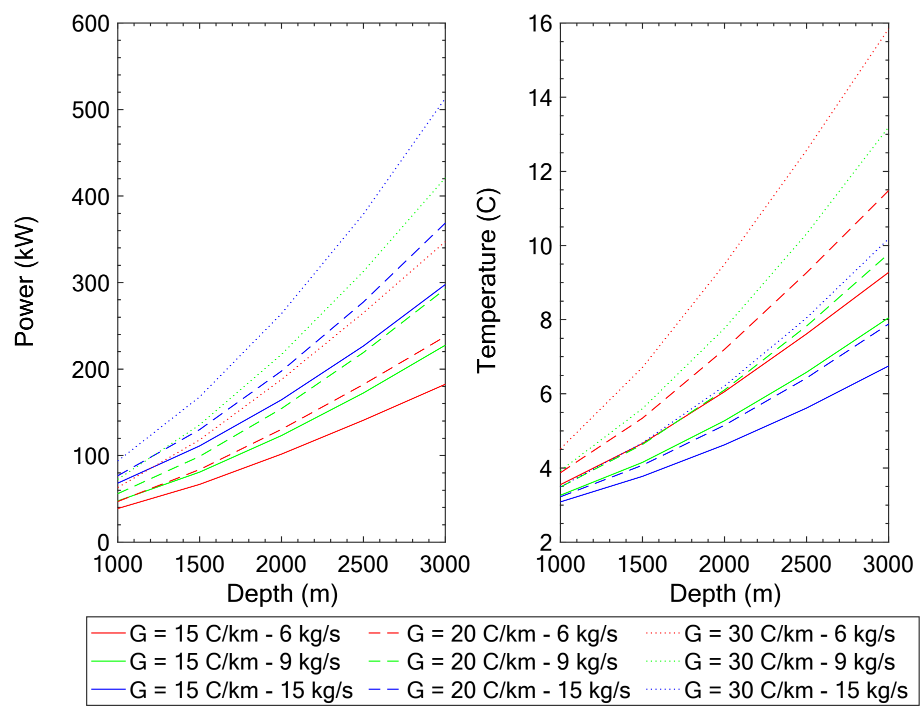

Fig. 7. Effect of the geothermal temperature gradient on the extracted power (left) and outlet temperature (right) from the DBHE well. $\lambda_g = 3$ W m^{-1} K^{-1}, $2r_1 = 90$ mm, $2r_2 = 200$ mm.

in the pipes, reduces when the mass flow rate increases, e.g., with 15 kg s^{-1} the effect is negligible between well or poorly insulated cases. Similarly, with wells less than 1500 m DBHE the effect is insignificant. However, with wells above 1500 m and at flow rates of 6 kg s^{-1} and 9 kg s^{-1}, the thermal short-circuiting of the fluids start to show an impact. For example, in a 3-km well and with 6 kg s^{-1} flow rate, the output power drops by 17 % and outlet temperature by ca 2 °C between a well and poorly insulated pipe. From a technical point of view, a well-insulated pipe would enable reducing the flow rate to reach the same performance than with a less insulated one. For example, in Fig. 6, U = 0.02 W m^{-1} K^{-1} and 6 kg s^{-1} corresponds to the output of U = 0.4 W m^{-1} K^{-1}and 9 kg s^{-1}. From an economic point of view, if an isolated inner pipe were expensive, raising the mass flow rate could be an option to compensate for the increased thermal short-circuiting.

As mentioned earlier, thermal short-circuiting may occur at lower flow rates, in which case the material used for the inner pipe plays a

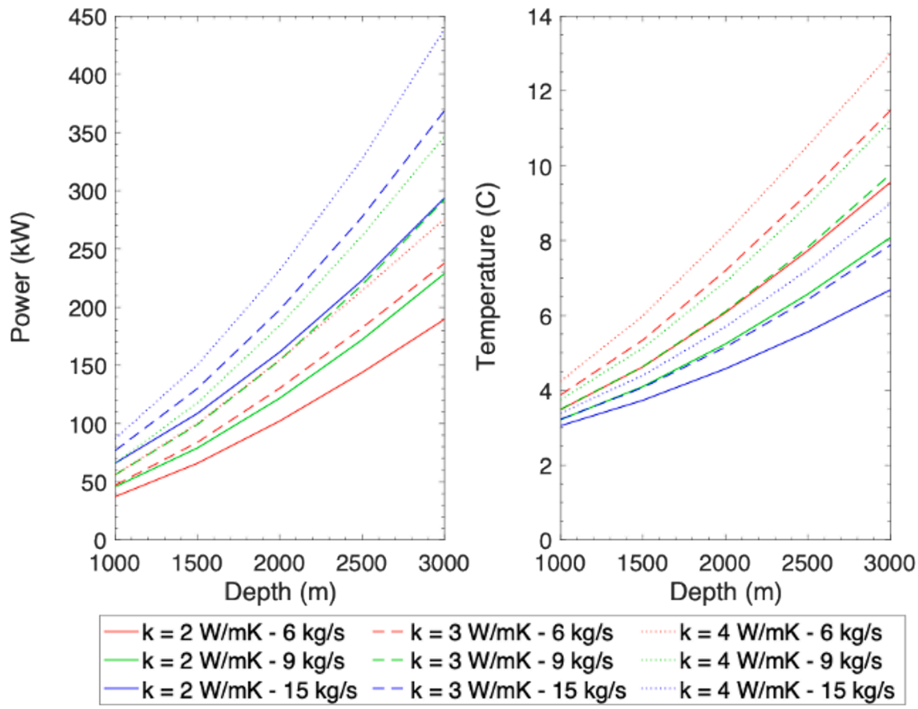

Fig. 8. Effect of thermal conductivity of ground on the power (left) and outlet temperature (right) from the DBHE. $2r_1 = 90$ mm, $2r_2 = 200$ mm, G = 20 °C km^{-1}. NB: thermal conductivity is denoted here with k.

significant role, i.e. using an isolating material would prevent thermal shunting. Also, if the mass flow rate is increased, the fluid velocity will increase helping to decrease the residence time of the fluid in the borehole, thereby reducing the risk of a thermal shunt.

4.2. Effect of geological parameters

The geothermal temperature gradient of ground varies geographically for which reason the effects of the gradient was investigated by analyzing the well performance for three gradient values: 15, 20, and 30 °C km^{-1}. Fig. 7 illustrates the results for the fixed reference geometry of the well as a function of the well depth and the mass flow rate as parameter, which demonstrates the importance of the gradient on the output thermal power and fluid temperature from the well. The effect of the mass flow rate increases with the depth of the well: In a 1-km DBHE with 6 kg s^{-1}, a 30 °C km^{-1} geothermal temperature gradient would deliver 63 % more thermal power than a 15 °C km^{-1} gradient, but the difference grows to 90 % at 3 km. Had the flow rate been 15 kg s^{-1}, the differences would have been 38 % and 72 %, respectively, which indicates that the effect of the mass flow rate gets more pronounced at larger depths. If focusing on the output power only, the effect of the thermal gradient could thus be compensated through a higher mass flow rate.

If striving for a certain output power from the well, a higher geothermal temperature gradient would require a shallower well leading to lower drilling costs of the well. The difference could be substantial, e.g., between 20 and 30 °C km^{-1} the required well depth could differ by from some hundred meters (high flow rate) to close to 1000 m (low flow rate).

Another benefit from a higher geothermal temperature gradient will be the higher outlet temperature of the fluid shown in Fig. 7 (right), which would positively affect the COP of the heat pump. The temperature effect is substantial and is pronounced at lower flow rates and deep wells. For example, for 6 kg s^{-1} and 2 km depth, the temperature difference would be 2.3 °C between the 20 and 30 °C km^{-1} geothermal temperature gradients.

The mass flow also affects the performance. In all cases, increasing the mass flow rate in the pipe will increase the heat extraction rate, but at the same time, the outlet temperature of the fluid from the borehole will decrease. At very high mass flow rates, the heat extraction rate will increase marginally only, and the temperature difference over the borehole will approach zero, which would not be practical for heating applications. In addition, higher flow rates will also cause higher pressure difference in the pipe.

Another important geological parameter is the thermal conductivity of the ground, which will affect the output power and the temperature from the well. In Fig. 8, λ_g is varied from 2 W m^{-1} K^{-1} to 4 W m^{-1} K^{-1}. The results show that irrespective of the mass flow rate in the well, a higher conductivity yields always a higher thermal power and outlet temperature from the well. For example, for 6 kg s^{-1} and 1000 m, doubling the thermal conductivity from 2 W m^{-1} K^{-1} to 4 W m^{-1} K^{-1} would increase the output by 51 %, but a higher flow rate of 15 kg s^{-1} would reduce the difference to 32 %. Increasing the well depth increases the difference at high mass flow rates, e.g., in the previous example to 49 %, but the relative difference reduces slightly at lower flow rates. The outlet temperature would also increase with increased conductivity as shown by Fig. 8 (right). For example, for 6 kg s^{-1} and 2 km depth, the temperature difference would be ca 2 °C between 2 W m^{-1} K^{-1} to 4 W m^{-1}K^{-1}.

4.3. Effect of heat pump system

In the previous sections, the thermal performance of the borehole heat exchanger (well) was evaluated in respect to the delivered thermal power from the ground and the outlet temperature from the well. The results from this analysis showed that the smaller inner pipe and a higher flow rate in the well gave the highest output.

In the next, the well is connected to a heat pump system to provide a whole systems view of the performance such as the effects on the COP of the heat pump and required pumping energy. The system to be evaluated consists of a single DBHE well connected to a heat pump and of a circulation pump-unit for the well. The outer diameter of the well is set to 200 mm and the heat pump parameters in Eq.(9) are $\eta_{CA} = 0.5$ and η_m

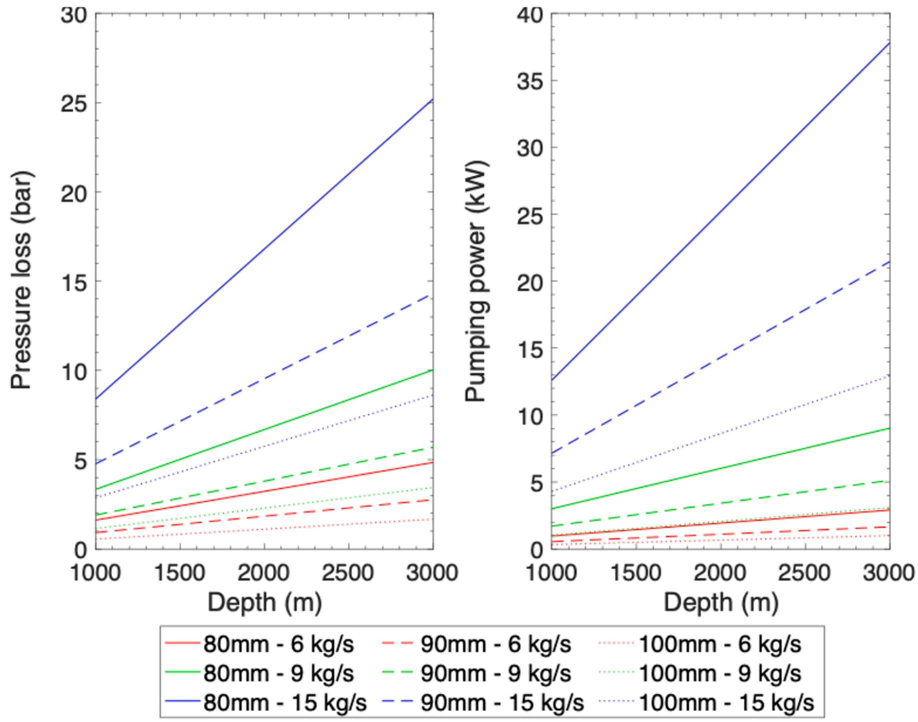

Fig. 9. Pumping power requirement with different mass flow rates and inner pipe diameters. $\lambda_g = 3$ Wm^{-1}K^{-1}, $2r_2 = 200$ mm, G = 20 °C km^{-1}.

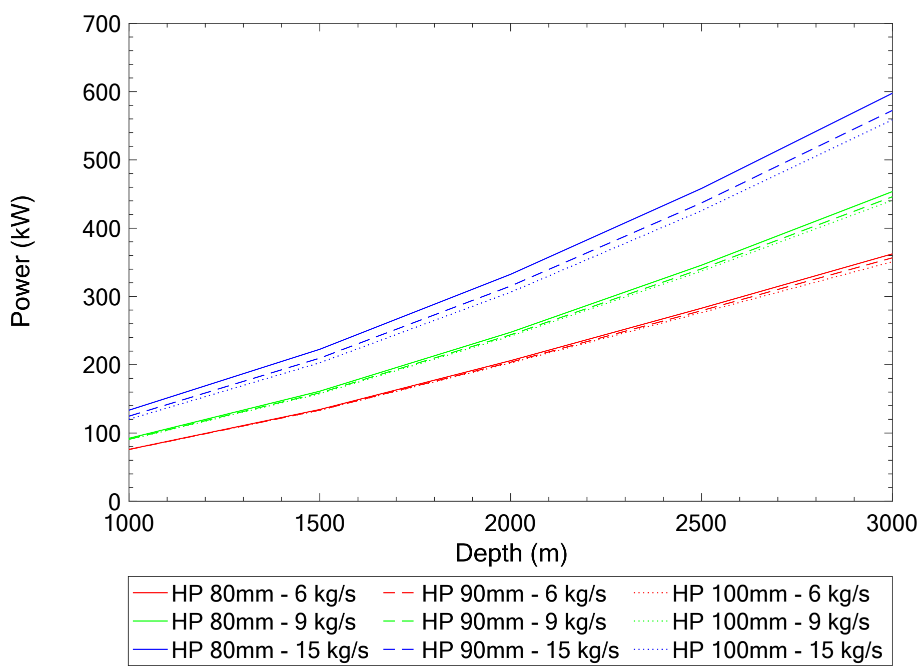

Fig. 10. Output power from the heat pump with a DBHE well. $\lambda_g = 3$ W m^{-1} K^{-1}, $2r_2 = 200$ mm, G = 20 °C km^{-1}.

= 0.9.

First, the pressure drop in the well and the pumping power required is analyzed in Fig. 9 as a function of the well depth and mass flow rate. At low mass flow rate (6 kg s^{-1}) and large pipe diameter (100 mm), the pressure losses are small, and the pumping power needed represent less than a few percent of the output power of the well; e.g., at 6 kg s^{-1} and with a 100 mm pipe for 1–3 km depths the share of the pumping power of the well output was 0.4 % – 0.3 % (from the top to the bottom of the borehole) and for a 80 mm pipe 1.3 % –0.8 % (see Fig. 5). However, with a higher flow rate (15 kg s^{-1}), the losses significantly increase, in particular with deeper wells and smaller pipe diameters. For example, with an 80 mm pipe the pumping power demand is twice that of the 90 mm pipe and 3–4-fold compared to the 100 mm pipe. The difference in the pumping power between 6 kg s^{-1} and 15 kg s^{-1} grows to an order of magnitude for deeper wells. Comparing to the thermal output in this case (Fig. 5) shows that the pumping power represents up to ca 10 % of the thermal power output of the well; e.g., at 15 kg s^{-1} and with an 80 mm pipe for 1000–3000 m depths the pumping power was 6–10 % of the output of the well and for a 100 mm pipe 2–4 %. Also, comparing Figs. 5 and 9 shows that the pumping power grows more steeply than the

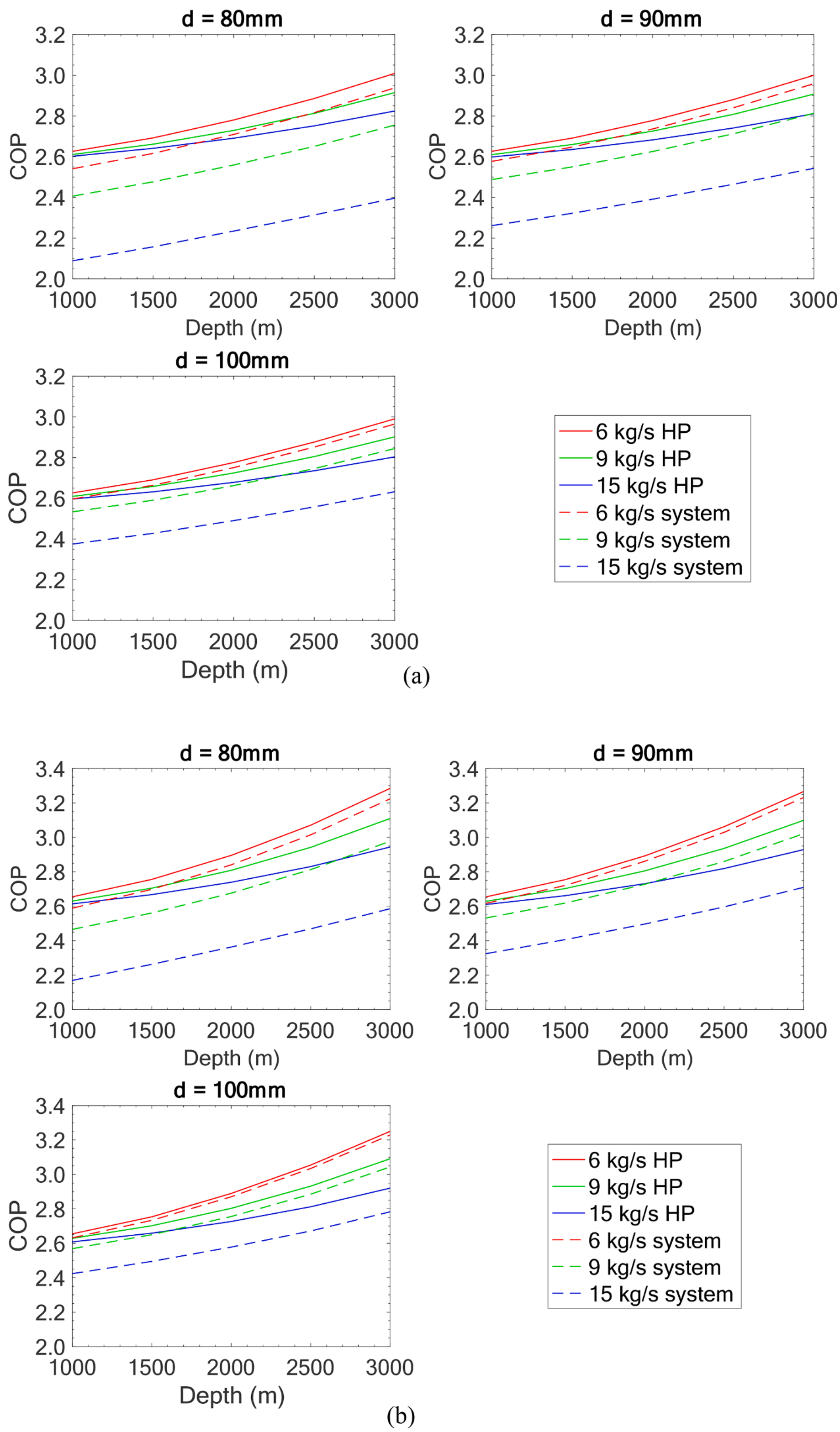

Fig. 11. Effect of mass flow rate on the heat pump and system COP. $\lambda_g = 3$ Wm^{-1}K^{-1}, $2r_1 = 80$ mm, $2r_2 = 200$ mm. (a) G = 20 °C km^{-1}, (b) G = 30 °C km^{-1}.

thermal output of the well as a function of the well depth and is also more sensitive to the inner diameter of the pipe.

Connecting next the heat pump to the system in Fig. 10, but neglecting the power demand of the circulation pump, shows that the performance differences between the flow rates are reduced. For example, at 6 kg s^{-1} and 9 kg s^{-1} flow rates the output from the heat pump remains almost the same irrespective the inner pipe diameter and well depth. This finding is independent of the magnitude of the geothermal temperature gradient. This is mainly explained by the dependence of the COP of the temperature levels. Also, the differences from the flow rates at lower well depths are smaller, but grow to 59 % (80 mm) and 64 % (100 mm) at 3 km depth, which is somewhat larger than without a heat pump (Fig. 5).

Finally, the power demand of the circulation pump for the well is also considered. The COP of the heat pump and the system COP (heat pump + pumping power) are shown in Fig. 11 for two geothermal temperature gradient cases as a function of the well depth using inner pipe diameter and mass flow rate as parameters. The effect of the pumping power can be found throughout the results, i.e., $COP_{system} < COP_{HP.}$ The difference gets pronounced at high flow rates (15 kg s^{-1}), e.g., with an 80 mm pipe and 2-km well the heat pump COP would be affected by ca 0.4-units due to the pumping losses, but is reduced to 0.2-units when a 100 mm pipe is employed. With a 6 kg s^{-1} flow rate, the effect is at most 0.1-units. Interestingly, the difference between the system and heat pump COP clearly diminishes with the well depth in the 15 kg s^{-1} case, which is explained by the higher outlet temperature from the pipe as more heat is extracted simultaneously. From the system point of view, the best efficiency is now reached with the larger pipe diameter (100 mm) and the lowest flow rate (6 kg s^{-1}), which minimizes the pressure drop in the well and the associated pumping power. However, from the application point of view, both the COP (Fig. 11) and the output power (Fig. 10) need to be considered simultaneously, because if just maximizing the COP of the system may lead to a thermal power deficit.

5. Conclusions

Deep borehole exchangers in the ground are a potential clean energy source for large-scale heating applications. Here a parametric study of such DBHE wells was undertaken to better understand how the well design and geological parameters would affect the thermal performance of the well. A numerical simulation model was employed in the analysis.

Key parameters used in the study included the diameter of the well, well depth, mass flow rate in the well and insulation between the inner and outer pipes in the well. Geological parameters included the geothermal temperature gradient and the thermal conductivity of the ground.

Based on the results of the analysis, it can be concluded that there is a cause-and-effect relationship between the different design parameters of the well. For example, when designing an optimal DBHE well, changing one parameter can e.g. lead to improved heat extraction, but it may also drop the temperature difference over the well, which may not necessarily be optimal for the heating system.

When considering the heat delivery of the DBHE well only, it was found that the spread of the well's thermal performance vis-à-vis the parameter values was wide. For example, for a 2-km well, the well design parameters could affect the thermal output by a factor of two. To maximize the output of the well, a high mass flow rate would be preferable. At high flow rates (15 kg s^{-1}), the effect of the insulation between the inner and outer pipes is very small. This is due to the increase in the fluid velocity which helps reducing the residence time of the water within the coaxial pipe, whereas at lower flow rates (6 kg s^{-1}), pipe insulation would clearly improve the performance with increasing depth to avoid thermal short-circuiting. For example, a 2-km well could yield 10 % more heat with an insulated inner pipe, but at 3 km even 20 %.

As to the ground parameters, a higher geothermal temperature gradient and a higher thermal conductivity would always improve the heat delivery of the well. Increasing λ_g from 2 W m^{-1} K^{-1} to 3 W m^{-1} K^{-1} (G = 20 °C km^{-1}) could yield 28 % more heat with a 2-km well and 6 kg s^{-1} flow rate and 22 % more with 15 kg s^{-1}. Increasing G from 20 to 30 °C km^{-1} (λ_g = 3 W m^{-1} K^{-1}) increases the heat output by 44 % with a 2-km well and 6 kg s^{-1} flow rate and 34 % more with 15 kg s^{-1}. The differences in λ_g and G for different sites could be compensated by the well depth and mass flow rate for a given output power level.

An important observation was that considering a DBHE heating system as a whole, the COP of the heat pump is affected by the fluid outlet temperature from the well, and the pumping power also need to be compensated for the pressure drop in the well. This has a major effect on the goodness of the system. The effect of the pumping power gets pronounced with a smaller pipe (80 mm) and higher flow rate (15 kg s^{-1}) and could drop the system COP by close to 0.5-units (heat pump COP 2.7 and system COP 2.2) for a 2-km well. Increasing the pipe diameter (100 mm) would drop the system COP much less, or, by 0.2-units.

Designing a DBHE well system with a heat pump and considering the hydraulic losses requires, however, a trade-off between the system COP and the output power from the well to meet the heating requirement of the application. Based on the results of this study, the following design guidelines could be recommended for different well depths in this respect:

Shallow wells <_1 km:

- A smaller inner pipe diameter (here 80 mm) and a reasonable mass flow rate (here 6 kg s^{-1}) is recommended, as a larger-diameter pipe (here 100 mm) would yield only marginally better system performance. Increasing the mass flow rate would increase the output power, but the system efficiency (COP) would decrease and enlarging the pipe diameter would be advisable.

Medium-deep borehole heat exchanger 1–1.5 km:

- A medium-sized inner pipe diameter (here 90 mm) yields a better system efficiency than a small pipe. A higher mass flow rate (here up to 15 kg s^{-1}) drops the system efficiency less than with shallow wells and could momentarily be used to increase output power, e.g., during peak demand.

Deep borehole heat exchangers > 1.5 km:

- A larger inner pipe diameter (here 100 mm) and a high mass flow rate (here 15 kg s^{-1}) are advised yielding higher output power. The differences in the system efficiencies (COP) between the different mass flow rates are small which supports higher flow rates.

It is important to pay attention to the geological conditions and parameters when planning a DBHE heating system, as the performance of the well is sensitive to both the thermal conductivity of the local ground and regional geothermal temperature gradient. Favorable geological conditions would often mean that a shorter well depth is adequate to meet the required thermal output and performance.

Though this study provides general design guidelines for designing DBHE well energy systems, which could well serve the pre-design of such systems, it should be noted that the final system design always requires careful planning case-by-case considering the local conditions and boundary conditions.

Declaration of competing interest

The authors declare that they have no known competing financial interests or personal relationships that could have appeared to influence the work reported in this paper.

Data availability

The authors do not have permission to share data.

References

[1] United Nations, Summary of the Paris Agreement, United Nations Framework Convention on Climate Change, 2015.

[2] C. Fetting, The European Green Deal, ESDN Report, Vienna, 2020 https://www.esdn.eu/fileadmin/ESDN_Reports/ESDN_Report_2_2020.pdf (accessed March 19, 2022).

[3] European Commission, Mapping and analyses of the current and future (2020 - 2030) heating/cooling fuel deployment (fossil/renewables). Executive summary, Brussels, 2020. https:/ec.europa.eu (accessed March 11, 2022).

[4] UN Environment, International Energy Agency, Towards a zero-emission, efficient, and resilient buildings and construction sector. Global Status Report 2017, 2017.

https://worldgbc.org/wp-content/uploads/2022/03/UNEP-188_GABC_en-web.pdf.
[5] Statistics Finland, Energy in Finland, Helsinki, 2021. https://www.tilastokeskus.fi/tup/julkaisut/tiedostot/julkaisuluettelo/yene_efp_202100_2021_23713_net.pdf (accessed March 19, 2022).
[6] Danish Energy Agency, Regulation and planning of district heating in Denmark, 2017. https://ens.dk/sites/ens.dk/files/Globalcooperation/regulation_and_planning_of_district_heating_in_denmark.pdf (accessed July 20, 2022).
[7] K. Johansen, S. Werner, Something is sustainable in the state of Denmark: A review of the Danish district heating sector, Renewable and Sustainable Energy Reviews 158 (2022) 112117, https://doi.org/10.1016/j.rser.2022.112117.
[8] S. Paiho, H. Saastamoinen, How to develop district heating in Finland? Energy Policy 122 (2018) 668–676, https://doi.org/10.1016/j.enpol.2018.08.025.
[9] City of Helsinki, Helsinki Energy Challenge: Background material – Heating system in Helsinki, Helsinki, 2020. https://www.hel.fi/static/kanslia/energy-challenge/heating-system-in-helsinki.pdf.
[10] P.D. Lund, K. Skytte, S. Bolwig, T.F. Bolkesjö, C. Bergaentzlé, P.A. Gunkel, J. G. Kirkerud, A. Klitkou, H. Koduvere, A. Gravelsins, D. Blumberga, L. Söder, Pathway analysis of a zero-emission transition in the Nordic-Baltic region, Energies (basel) 12 (2019) 3337.
[11] International Energy Agency, Heat pumps, Paris, 2021. https://www.iea.org/energy-system/buildings/heat-pumps (accessed March 28, 2022).
[12] J. Hirvonen, J. Jokisalo, P. Sankelo, T. Niemelä, R. Kosonen, Emission reduction potential of different types of Finnish buildings through energy retrofits, Buildings 10 (2020) 234, https://doi.org/10.3390/buildings10120234.
[13] J.M. Lattimer, M. Prakash, Heat from renewable energy sources: The RES-H initiative and related directives, Delft, 2002. https://climate.ec.europa.eu/system/files/2016-11/renewable_energy_srcs_heat_en.pdf (accessed March 17, 2022).
[14] I. Sarbu, C. Sebarchievici, General review of ground-source heat pump systems for heating and cooling of buildings, Energy Build 70 (2014) 441–454, https://doi.org/10.1016/j.enbuild.2013.11.068.
[15] S. Kubba, Handbook of Green Building Design and Construction: LEED, BREEAM, and Green Globes, Elsevier, 2017 https://www.sciencedirect.com/book/9780128104330/handbook-of-green-building-design-and-construction (accessed March 11, 2022.
[16] S.E. Gehlin, J.D. Spitler, G. Hellström, Deep boreholes for ground source heat pump systems – Scandinavian experience and future prospects, in: ASHRAE Winter Meeting, American Society of Heating, Refrigerating and Air-Conditioning Engineers (ASHRAE), Orlando, 2016.
[17] K. Korhonen, N. Leppäharju, P. Hakala, T. Arola, Simulated temperature evolution of large BTES – case study from Finland, in: Proceedings of the IGSHPA Research Track 2018, Stockholm, 2019. https://doi.org/10.22488/okstate.18.000033.
[18] J. Kallio, K. Korhonen, M. Wennerström, O. Sallasmaa, I. Witick, I. Vähäaho, R. Niinimäki, P. Leivo, J. Peura, Helsingin geoenergiapotentiaali (Geoenergy potential of Helsinki) Kaupunkiympäristön julkaisuja 2019: 25 (Publications of city planning), accessed March 11, 2022, Helsinki (2019), https://ahjojulkaisu.hel.fi/5C198802-3A15-C2D1-944C-725ACE400000.pdf.
[19] K. Piipponen, A. Martinkauppi, K. Korhonen, S. Vallin, T. Arola, A. Bischoff, N. Leppäharju, The deeper the better? A thermogeological analysis of medium-deep borehole heat exchangers in low-enthalpy crystalline rocks, Geothermal Energy (heidelberg) 10 (2022) 1–20, https://doi.org/10.1186/s40517-022-00221-7.
[20] T. Kohl, R. Brenni, W. Eugster, System performance of a deep borehole heat exchanger, Geothermics 31 (2002) 687–708, https://doi.org/10.1016/S0375-6505(02)00031-7.
[21] Z. Wang, F. Wang, J. Liu, Z. Ma, E. Han, M. Song, Field test and numerical investigation on the heat transfer characteristics and optimal design of the heat exchangers of a deep borehole ground source heat pump system, Energy Convers Manag 153 (2017) 603–615, https://doi.org/10.1016/j.enconman.2017.10.038.
[22] A. Lund, Analysis of deep-heat energy wells for heat pump systems, Aalto University, M.Sc.Tech.Thesis, 2019.
[23] E. Zanchini, S. Lazzari, A. Priarone, Improving the thermal performance of coaxial borehole heat exchangers, Energy 35 (2010) 657–666, https://doi.org/10.1016/j.energy.2009.10.038.
[24] Y. Luo, H. Guo, F. Meggers, L. Zhang, Deep coaxial borehole heat exchanger: Analytical modeling and thermal analysis, Energy 185 (2019) 1298–1313, https://doi.org/10.1016/j.energy.2019.05.228.
[25] H. Holmberg, J. Acuña, E. Næss, O.K. Sønju, Thermal evaluation of coaxial deep borehole heat exchangers, Renew, Energy 97 (2016) 65–76, https://doi.org/10.1016/j.renene.2016.05.048.
[26] K.H. Kvalsvik, K. Midttømme, R.K. Ramstad, Geothermal energy use, country update for Norway, in: European Geothermal Congress 2019, Den Haag, 2019. https://europeangeothermalcongress.eu/wp-content/uploads/2019/07/CUR-20-Norway.pdf (accessed March 22, 2022).
[27] T. Arola, M. Wiberg, Geothermal energy use, country update for Finland, in: European Geothermal Congress 2022, Berlin, 2022.
[28] W. Cai, F. Wang, J. Liu, Z. Wang, Z. Ma, Experimental and numerical investigation of heat transfer performance and sustainability of deep borehole heat exchangers coupled with ground source heat pump systems, Appl Therm Eng 149 (2019) 975–986, https://doi.org/10.1016/j.applthermaleng.2018.12.094.
[29] H. Lund, B. Möller, B.V. Mathiesen, A. Dyrelund, The role of district heating in future renewable energy systems, Energy 35 (2010) 1381–1390, https://doi.org/10.1016/j.energy.2009.11.023.
[30] R.N. Horne, Design consideration of a down-hole coaxial geothermal heat exchanger, in: Transactions - Geothermal Resources Council, Geothermal Resource Council, Salt Lake City, 1980.
[31] C. Rindahl, Geothermal energy: Model development and analysis of a pilot project, Master's Thesis, Norwegian University of Science and Technology, Department of Energy and Process Engineering, 2016.
[32] K. Bär, W. Rühaak, B. Welsch, D. Schulte, S. Homuth, I. Sass, Seasonal high temperature heat storage with medium deep borehole heat exchangers, Energy Procedia (2015) 351–360, https://doi.org/10.1016/j.egypro.2015.07.841.
[33] F.P. Incropera, D.P. Dewitt, Fundamentals of Heat and Mass Transfer, 5th ed., Wiley, 2001.
[34] M.V. Lurie, Modeling of Oil Product and Gas Pipeline Transportation, Wiley (2008), https://doi.org/10.1002/9783527626199.
[35] V. Gnielinski, New Equations for Heat and Mass Transfer in Turbulent Pipe and Channel Flow, International Chemical Engineering 16 (1976) 8–16.
[36] A. Huusko, Geologian tutkimuskeskus kartoittaa Suomen geoenergiapotentiaalia (Geololical Survey of Finland maps the geoenergy potential of Finland), Positio, accessed February 18, 2022, Maanmittauslaitos (2016) 12–15, https://www.gtk.fi/ajankohtaista/suomen-keskisyva-geoterminen-energiapotentiaali-maaritetty-avaa-mahdollisuuksia-vahahiilisen-lammitysenergian-hyotykayttoon-taajama-alueilla/.
[37] A. Nador, Danube Region Geothermal Report, 2014. www.danube-energy.eu (accessed March 17, 2022).
[38] COMSOL, COMSOL Multiphysics®, (n.d.), Version 6.0.
[39] L. Eskola, K. Siren, J. Jokisalo, Lämpöpumppujen energialaskentaopas (Guide for energy assessment of heat pumps), Helsinki, 2012. http://www.ymparistoministerio.fi/fi-FI/Maankaytto_ja_rakentaminen/Lainsaadanto_ja_ohjeet/Rakentamismaarayskokoelma (accessed March 8, 2022).
[40] A. Laitinen, P. Tuominen, R. Holopainen, P. Tuomaala, J. Jokisalo, L. Eskola, K. Sirén, Renewable energy production of Finnish heat pumps: Report of the SPF-project, VTT Technical Research Centre of Finland, Espoo, 2014.
[41] P. Lund, Studies on solar heating systems with long-term heat storage for northern high latitudes, Applied Physics Series, Acta Polytechnica Scandinavica, 1984, pp. 1–35.
[42] F.M. White, Fluid Mechanics, 7th Edition, McGraw-Hill, New York, 2011.
[43] G.J. Jung, G.S. Oh, C.W. Chung, H.J. Kim, Heat transfer on grooved high density poly ethylene tube for surface water source heat pump, Thermal Science 18 (2014) 1327–1341, https://doi.org/10.2298/TSCI130513017J.
[44] S. Peltoniemi, I. Kukkonen, Kivilajien lämmönjohtavuus Suomessa (Thermal conductivity of different rock types), Report Q18/95/1, Espoo, 1995.
[45] C. Clauser, E. Huenges, Thermal Conductivity of Rocks and Minerals, in: Rock Physics and Phase Relations. A Handbook of Physical Constants, 1995.
[46] P. Baillieux, Multidisciplinary approach to understand the localization of geothermal anomalies in the Upper Rhine Graben from regional to local scale, University of Neuchâtel, 2012. Doctoral Thesis.
[47] M. Macenić, T. Kurevija, I. Medved, Novel geothermal gradient map of the Croatian part of the Pannonian Basin System based on data interpretation from 154 deep exploration wells, Renewable & Sustainable Energy Reviews 132 (2020) 110069, https://doi.org/10.1016/j.rser.2020.110069.
[48] S. Sliaupa, G. Motuza, L. Korabliova, K. Ciuraite, V. Puronas, Geothermal Potential of Hot Granites of Lithuania, Proceedings World Geothermal Congress 2010 Bali, Indonesia, 25-29 April 2010 (2010).
[49] M. Labus, K. Labus, Thermal conductivity and diffusivity of fine-grained sedimentary rocks, Journal of Thermal Analysis and Calorimetry 132 (2018) 1669–1676, https://doi.org/10.1007/s10973-018-7090-5.
[50] M.R. Gillespie, E.J. Crane, H.F. Barron, Deep geothermal energy potential in Scotland. British Geological Survey Commissioned Report, CR/12/131, 129pp, 2013.
[51] W. Huang, J. Chen, J. Cen, W. Cao, Z. Li, F. Li, F. Jiang, Heat extraction from hot dry rock by super-long gravity heat pipe: Effect of key parameters, Energy 248 (2022) 123527.
[52] R.C. Selley, L.R.M. Cocks, I.R. Plimer (Eds.), Encyclopedia of Geology, Elsevier, Reference Work, 2005.
[53] K. Senger, M. Nuus, N. Balling, P. Betlem, T. Birchall, H.H. Christiansen, H. Elvebakk, S. Fuchs, M. Jochmann, P. Klitzke, K. Midttømme, S. Olaussen, C. Pascal, N. Rodes, A. Shestov, A. Smyrak-Sikora, P.J. Thomas, The subsurface thermal state of Svalbard and implications for geothermal potential, Geothermics 111 (2023) 102702.